Characterization of coprecipitated aluminium–chromium mixed hydroxides and of the products of their calcination

Josè Manuel Gallardo Amores,[a†] Maria del Carmen Prieto,[a] Vicente Sanchez Escribano,[a] Cinzia Cristiani,[b] Marcella Trombetta[c] and Guido Busca*[c]

[a]*Departamento de Quimica Inorganica, Universidad, Placa de la Merced, E-37008 Salamanca, Spain*

[b]*Dipartimento di Chimica Industriale e Ingegneria Chimica 'Giulio Natta', Politecnico di Milano, P.le Leonardo da Vinci 23, 20122 Milano, Italy*

[c]*Istituto di Chimica, Facoltà di Ingegneria, Università, P.le Kennedy, I-16129 Genova, Italy*

Crystalline phases have been coprecipitated from Al/Cr mixed-nitrate aqueous solutions with ammonium carbonate. These phases have been characte rized as probably layered hydroxycarbonates with the likely composition $(NH_4)_2(Al,Cr)_6(OH)_{14}(CO_3)_3{\cdot}H_2O$, using XRD, FTIR and TG–DTA analyses. The calcination of these materials gives rise to amorphous mixed oxides where Cr is partly in the hexavalent state, while further calcination at 1173 K gives rise to polyphasic materials. Samples with Al: Cr atom ratio between 5 : 1 and 1 : 1 give rise to four phase materials with three corundum-type phases and a spinel-type phase. All these phases contain both Al and Cr.

Introduction

Alumina–chromia mixed oxides have been used for decades as catalysts for the dehydrogenation of alkanes to the corresponding alkenes.[1] This technology underwent new emphasis in recent years due to the availability of light alkanes arising from natural gas and to its improvement owing to the appearance of new reactor designs[2] and is focusing much interest in particular in relation to the possibility to synthesize isobutene from isobutane dehydrogenation. Catalysts can be either produced by impregnation of alumina supports with chromium compounds or by coprecipitation of Cr and Al mixed hydroxy compounds, followed by calcination. Data concerning catalyst preparation and characterization have been discussed extensively.[3]

On the other hand, the Al_2O_3–Cr_2O_3 system is also of practical interest for other reasons. Powders belonging to this system active in heterogeneously catalyzed processes aimed at reduction of air pollution,[4,5] can form under high-temperature corrosion of Fe–Cr–Al alloys[6] and can be precursors for alumina–chromium nanocomposites[7] as well as being useful in paint technology.[8]

The solid-state chemistry of the Al_2O_3–Cr_2O_3 system has also been investigated extensively. The thermodynamically stable phases of chromia (α-Cr_2O_3, eskolaite) and alumina (α-Al_2O_3, corundum) are isostructural with each other and with hematite (α-Fe_2O_3), all crystallizing in the rhombohedral–hexagonal system, with space group $R3c$ and $Z = 6$.[9] However, thermodynamically stable solid solutions exist in the entire compositional range and at any temperature only between α-Fe_2O_3 and α-Cr_2O_3. In the case of the Al_2O_3–Cr_2O_3 system, complete miscibility is limited to high temperatures,[10] a miscibility gap appearing below 1573 K.[11] On the other hand, iron and aluminium oxides can also form metastable sesquioxides (γ-Al_2O_3, δ-Al_2O_3, θ-Al_2O_3, η-Al_2O_3 and γ-Fe_2O_3) whose structure is related to that of spinel ($MgAl_2O_4$), owing to the ability of their trivalent cations Al^{3+} (d^0) and Fe^{3+} (d^5) to occupy tetrahedral sites. These phases have important applications in catalysis. On the contrary, Cr^{3+} (d^3) occupies tetrahedral sites only with difficulty, owing to the very high crystal field stabilization energy of such sites.[9] Accordingly, chromium sesquioxides with spinel-related structures are virtually non-existent, although possibly impure phases denoted as γ-Cr_2O_3[12] and η-Cr_2O_3[13] have been reported. Moreover, there are conflicting opinions on the solubility of chromia in such metastable aluminas.[4,14]

In previous papers we investigated powders belonging to the Fe_2O_3–Cr_2O_3 system[15,16] and to the Al_2O_3–Fe_2O_3 system[17,18] and the surface properties of corundum and spinel-type metal oxides.[19] We characterized metastable Fe_2O_3–Cr_2O_3 solid solutions with ilmenite-type superstructure,[16] metastable Fe_2O_3–Al_2O_3 corundum-type solid solutions with compositions external to the thermodynamic solubility limits[18] and spinel-type Fe_2O_3–Al_2O_3 solid solutions.[19] We present here a preparation and characterization study of materials belonging to the Al_2O_3–Cr_2O_3 system, in the side rich in Al. The aim was to complete the study of mixed oxide powders of trivalent metals and to gain experience in the preparation chemistry of alumina–chromia dehydrogenation catalysts.

Experimental

Preparation procedure

The precursor powders were prepared by a coprecipitation procedure similar to that used previously,[15,17,18] at pH = 9 from mixed aqueous solutions of $Cr(NO_3)_3{\cdot}9H_2O$ and $Al(NO_3)_3{\cdot}9H_2O$ by addition of NH_3–$(NH_4)_2CO_3$. The powders were aged in contact with the solution for 3 days at 333 K. After filtering, the precipitates were washed carefully and dried at 393 K for 3 h. The mixed oxides were produced by calcination of the precursors in air at 673 K and at 1173 K for 5 h. For the pure aluminium phase, the precipitation was repeated using a larger excess of $(NH_4)_2CO_3$ and no NH_3. All reagents were from Carlo Erba (Milano, Italy).

The samples studied here are denoted Al, Al5Cr1, Al2Cr1, Al1Cr1 and Cr, with Al to Cr atomic ratios of ∞, 4.8, 2.3, 1.3 and 0, respectively, as measured by plasma emission spectrometry. For the mixed oxides the above notation is used followed by the calcination temperature in K.

Characterization procedures

XRD analyses were performed with a Philips model PW 1130–1049/10 (Co-Kα radiation) and a Siemens 500 (Cu-Kα

† Present Address: Departamento de Ciencia de Materiales, Facultad de Quimicas, Universidad Complutense, Ciudad Universitaria, E-28040 Madrid, Spain.

radiation) instrument. Elemental analyses were carried out with a Plasma II Perkin Elmer emission spectrometer after dissolution in $HF–HNO_3$. Diffuse reflectance UV–VIS spectra were recorded with a Hewlett-Packard 8452-A diode ray spectrometer.

TG–DTA analyses performed in air ($10\,K\,min^{-1}$) were recorded on a Setaram T92 apparatus. The IR spectra were recorded by a Nicolet Magna 750 Fourier-transform instrument. For the skeletal spectra, KBr pressed disks and a beam splitter were used in the region above $400\,cm^{-1}$. The region $400–50\,cm^{-1}$ was recorded using a 'solid substrate' beam splitter, with the powder deposed over a polyethylene disk.

Results and Discussion

Characterization of the precipitates

XRD analysis of the Cr-free Al precipitate [Fig. 1(a)] clearly shows broad diffraction peaks of boehmite γ-AlOOH (JCPDS no. 21–1307) corresponding to interplanar distances (d) at *ca.* 6.10, 3.20, 2.34 and 1.86 Å. However, additional sharp peaks were observed, reported in Table 1, and correspond to a different phase.

For the mixed Al–Cr precipitates [Fig. 1(b)–(d)] a well defined XRD pattern appears, composed of sharp peaks; this indicates the existence of highly crystalline phases, the crystallinity of which, however, decreases upon increasing the Cr content. These peaks (Table 1) correspond to the sharp peaks observed in the XRD pattern of the pure Al precipitate. However, upon reference to JCPDS files, the overall pattern does not seem to be consistent with those of any known hydroxide and/or oxide of chromium and/or of aluminium. However, a similar pattern was previously cited in work concerning Al–hydroxide precipitates by Vogel *et al.*[20] and by Groppi *et al.*[21] According to these authors this phase corresponds to a composition $(NH_4)_2Al_6(OH)_{14}(CO_3)_3{\cdot}H_2O$, *i.e.* a hydroxycarbonate of Al and ammonium.

To obtain more precise information, we repeated the preparation of Groppi *et al.*[21] using a larger excess of $(NH_4)_2CO_3$ and we obtained this phase, almost pure, with the XRD pattern shown in Fig. 2. The positions of the XRD peaks assigned to these hydroxycarbonate phases are compared in Table 1. Continuous shifts of the diffraction peaks and the corresponding expansion of the interplanar distances upon increasing the Cr content suggests that Cr substitutes for Al in this structure, and, finally, a true mixed hydroxycarbonate precipitate. We tentatively assign the observed phases as $(NH_4)_2(Al,Cr)_6(OH)_{14}(CO_3)_3{\cdot}H_2O$ solid solutions, in agreement with Vogel *et al.*[20] and Groppi *et al.*[21] The XRD patterns seem consistent with those of layered compounds.

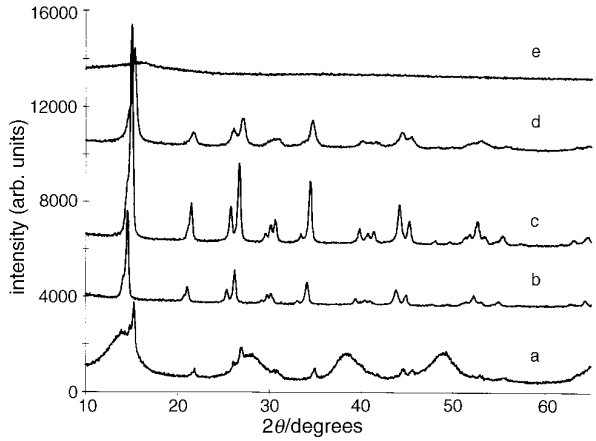

Fig. 1 XRD patterns of the precipitates (a) Al, (b) Al5Cr1, (c) Al2Cr1, (d) Al1Cr1, (e) Cr

The pure Cr precipitate, prepared under the same conditions for comparison, is totally amorphous by XRD [Fig. 1(e)].

To obtain further evidence of the assigned composition we performed FTIR and TG analyses. FTIR spectra of the crystalline mixed Al–Cr precipitates are shown in Fig. 3, and tentative assignments of the observed bands are reported in Table 2. These assignments are proposed by comparison with the spectra of inorganic compounds (hydroxides, carbonates, nitrates and ammonium salts[22,23]), including those of Al hydroxides and oxyhydroxides,[22,24] of bulk and surface carbon-

Table 1 Interplanar distances calculated from the XRD peaks of the $(NH_4)_2(Al,Cr)_6(OH)_{14}(CO_3)_3{\cdot}xH_2O$ phases in the chromium–aluminium coprecitates

Al1Cr1		Al2Cr1		Al5Cr1		Al preparation I[a]	Al preparation II	
d/Å	I_{rel}	d/Å	I_{rel}	d/Å	I_{rel}	d/Å	d/Å	I_{rel}
6.3344	32.8	sh		sh		6.2935		
6.0853	100.0	5.8992	100.0	5.7753	100.0	5.7974	5.7913	100.0
4.2181	21.8	4.1354	20.5	4.0953	20.8	4.0703	4.0753	20.2
3.5124	19.1	3.4437	18.8	3.4119	24.7	3.4148		
3.3968	39.0	3.3375	38.4	3.2925	34.2	3.3077	3.3078	33.3
3.0589	8.1	3.0218	6.9	2.9976	12.7	2.9968		
3.0047	14.0	2.9633	10.7	2.9339	14.9	2.9304	2.9046	12.7
2.9607	15.0	2.9151	13.1	2.8961	14.4		2.8616	14.0
2.7066	7.7	2.6751	6.9					
2.6257	26.6	2.5999	30.4	2.5826	32.6	2.5624	2.5559	20.2
2.2904	10.0	2.2655	9.1	2.2494	13.2			
2.2336	8.9	2.2153	7.1			2.1939	2.1876	5.2
2.2052	8.0	2.1842	7.8	2.1722	12.7	2.1602		
2.0688	19.2	2.0519	19.8	2.0408	21.3	2.0326	2.0372	15.4
2.0209	13.6	2.0061	12.6	1.9983	17.3	1.9903		
		1.8951	4.1					
1.8435	5.0	1.8354	4.0					
1.7768	7.29	1.7788	5.7					
		1.7646	7.0					
1.7504	14.1	1.7378	12.6	1.7267	14.2	1.7296	1.7353	8.7
1.7260	7.3	1.7159	6.0					
1.6752	7.6	1.6579	6.3			1.6514	1.6539	3.4
1.4789	5.2	1.4733	4.4				1.4689	2.8
1.4468	9.0	1.4408	5.7				1.4312	9.5

[a]In the case of preparation I the relative intensities could not be measured because of superimposition with peaks of boehmite. [b]sh = shoulder.

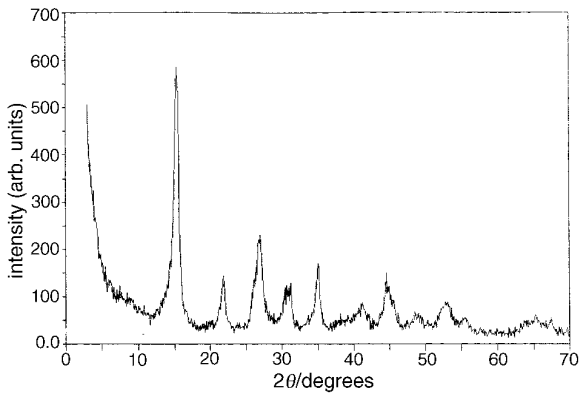

Fig. 2 XRD pattern of the pure Al precipitate, second preparation

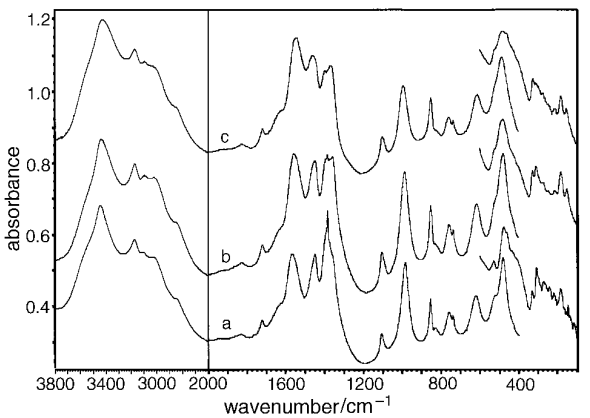

Fig. 3 FTIR spectra of the mixed Al–Cr precipitates (a) Al5Cr1, (b) Al2Cr1, (c) Al1Cr1

ate complexes[25] and of other Al-containing hydroxycarbonates.[26] The IR spectra demonstrate that the samples are constituted by hydroxides that also contain ammonium ions and carbonate and/or nitrate ions. Nitrate ions are certainly present in Al5Cr1, while they are certainly much less abundant for Al2Cr1 and are virtually absent for Al1Cr1.

TG analyses (Fig. 4) show that these materials first lose mass in the range 373–493 K and then decompose in the temperature range 493–593 K. Simultaneously recorded DTA analyses show that both these losses correspond to endothermic peaks. In the first step the mass loss is of the order 10% for all three precipitates, while in the second decomposition step the mass loss increases in the sequence Al1Cr1 < Al2Cr1 < Al5Cr1, and is in the range 40–50%. Assuming that the first step is essentially due to the desorption of adsorbed water and/or CO_2 species, and that the second step involves a true decomposition reaction, these data are in accord with the above formula. In fact, the theoretical mass losses upon the following decomposition reaction:

$$(NH_4)_2(Al,Cr)_6(OH)_{14}(CO_3)_3\cdot H_2O \rightarrow 3(Al,Cr)_2O_3 + 2NH_3 + 3CO_2 + 9H_2O$$

are 49% for Al5Cr1, 47% for Al2Cr1 and 45% for Al1Cr1. However, IR spectra show that carbonates can be substituted in part by nitrates in the Al-rich precipitates. An additional small mass loss is detected at 823 K and is strongest for the sample richest in Cr (Al1Cr1). This can be assigned to a

Table 2 Position (wavenumbers, cm^{-1}) of the IR bands in the spectra of the $(NH_4)_2(Al,Cr)_6(OH)_{14}(CO_3)_3\cdot xH_2O$ precipitates

				assignment	
Al(II)	Al5Cr1	Al2Cr1	Al1Cr1	mode	species
(3560)	3580 (sh)	3570 (sh)	3560 (sh)	ν(OH)	OH
3446	3447	3438	3429	ν(OH)	OH
3180	3175	3173	3174	$\nu(NH_4)$	NH_4^+
3105	3109	3097	3098	$\nu(NH_4)$	NH_4^+
3040	3034	3023	3015 (sh)	$\nu(NH_4)$	NH_4^+
2880	2859	2855 (sh)	2850 (sh)	$\nu(NH_4)$	NH_4^+
1721	1723	1721	1719	$\delta_{as}(NH_4)$	NH_4^+
1620	1615 (sh)	1615 (sh)	1615 (sh)	$\delta(OH_2)$	H_2O
1558	1566	1559	1542	ν(CO)	CO_3^{2-}
1455	1449	1448	1457	$\delta_{sym}(NH_4)$	NH_4^+
	1400 (sh)	1398	1397	ν(CO)	CO_3^{2-}
1392	1385	1384		ν(NO)	NO_3^-
1360	1360 (sh)	1365	1367	ν(CO)	CO_3^{2-}
1107	1107	1106	1104	δ(OH)	OH
988	984	986	995	δ(OH)	OH
854	852	852	852	δ(OCO)	CO_3^{2-}
	830	832	830	δ(ONO)	NO_3^-
	757	757	758		
738	737	735	735		
624	620	615	612		
	529 (sh)	530 (sh)	530 (sh)		
482	480	481	487		
	400 (br)			Al—O	
	330	327	325	Cr—O	
	307	309	310		
	271	273	270		
	241	246		lattice modes	
	218	216	215		
	184	182	181		
	146	151	153		

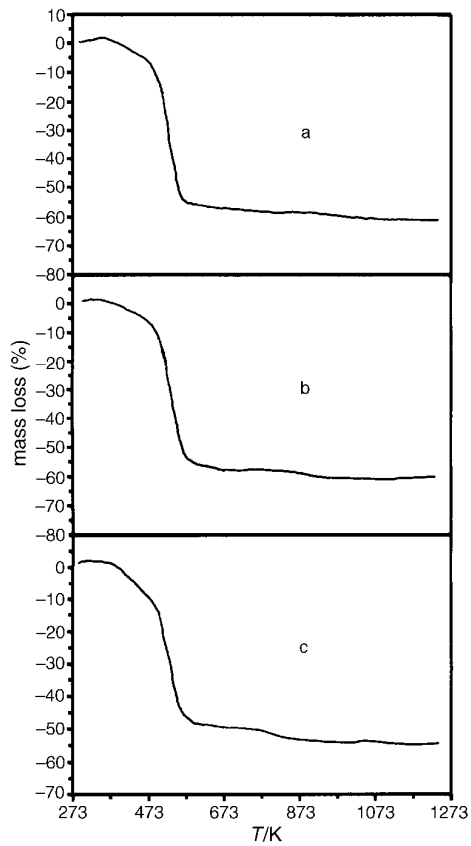

Fig. 4 Thermogravimetric curves of the mixed Al–Cr precipitates (a) Al5Cr1, (b) Al2Cr1, (c) Al1Cr1

Table 3 Interplanar distances calculated from the XRD peaks of the α-$(Cr,Al)_2O_3$ hexagonal–rhombohedral phases in the chromia–alumina samples treated at the temperatures shown

		Cr		Cr1Al1			Cr1Al2				Cr1Al5			Al	
		673 K	1173 K	673 K	1173 K		673 K	1173 K			1173 K			1173[c] K	
hkl	α-Cr_2O_3[a]				α_1	α_3		α_1	α_2	α_3	α_1	α_2	α_3		α-Al_2O_3[b]
012	3.6312	3.7319	3.6739	3.6019	3.6154		3.5750	3.6340			3.6018				
						3.5529				3.5529		3.5861	3.5377	3.5156	3.479
104	2.6649	2.7142	2.6846	2.6450	2.6530		2.6372	2.6630			2.6626				
						2.5942				2.6082		2.6256	2.5881	2.5671	2.552
110	2.4794	2.5170	2.4945	2.4620	2.4698		2.4525	2.4792			2.4695				
									2.4729			2.4529			
						2.4093				2.4311			2.4181	2.3943	2.379
113	2.1753	2.2017	2.1866	2.1605	2.1657		2.1519	2.1684			2.1694				
									2.1350			2.1428			
						2.1157				2.1234			2.1145	2.0959	2.085
024	1.8156	1.8339	1.8220	1.8046	1.8070		1.7968	1.8126			1.8116				
									1.7967			1.7919			
						1.7680				1.7737			1.7675	1.7468	1.740
116	1.6725	1.6854	1.6786	1.6623	1.6655		1.6594	1.6701			1.6686				
									1.6559			1.6494			
						1.6250				1.6278			1.6243	1.6072	1.601
018	—	1.5924	1.5841	1.5696	1.5729		—	1.5716							
									1.5599			1.5368			
						1.5331				1.5348				masked	1.510
214	1.4649	1.4744	1.4682	1.4573	1.4548		1.4544	1.4625			1.4597				
									1.4460						
						1.4485				1.4375			1.4288	masked	1.404
300	1.4317	1.4393	1.4331	1.4237	1.4219		—[d]	1.4171			1.4062				
									1.4147						
						1.3900				1.4073			1.3961	masked	1.374

[a]JCPDS file 38-1479 (synthetic eskolaite). [b]JCPDS file 42-1468 (corundum). [c]Minor phase, θ-Al_2O_3 is the major phase. [d]Uncertain position.

thermal decomposition of a chromium(VI) oxo species to chromium(III) oxide, with loss of oxygen (see below).

These data allow us to conclude that layered hydroxycarbonates of Al, Cr and ammonium have been prepared, with the general approximate formula

$$(NH_4)_2(Al,Cr)_6(OH)_{14}(CO_3)_3{\cdot}H_2O$$

Characterization of mixed oxides produced by calcination at 673 K

The XRD patterns of the mixed-oxide samples produced by calcination at 673 K of the above-described precipitates are shown in Fig. 5. The very broad pattern of the pure Al sample is typical for a poorly crystalline defective spinel-type phase γ-Al_2O_3.[27,28] The decomposition of $(NH_4)_2Al_6(OH)_{14}(CO_3)_3{\cdot}H_2O$ to γ-Al_2O_3 has already been reported both by Vogel *et al.*[20] and by Groppi *et al.*[21] Sample Al5Cr1-673 appears to be completely amorphous while the pattern of the sample Al2Cr1-673 is almost completely amorphous, although by strongly expanding the ordinate scale, traces of a corundum-type phase can be seen. On the other hand, sample Al1Cr1-673 is well crystallized in a corundum-type structure isomorphous to both α-Cr_2O_3 and α-Al_2O_3. This phase appears to be even better crystallized than a sample obtained by calcination at 673 K of amorphous Cr hydroxide. Table 3 lists XRD peak positions of these corundum-type phases along with those of reference compounds while Table 4 lists unit-cell parameters calculated from these data. It is evident that the peak position, crystal plane distances and unit-cell parameters indicate that the sample Al1Cr1-673 is a solid solution. No extra peaks are observed, so that no evidence is found for a superstructure arising from Al and Cr cation ordering. Thus, it is assumed that the cation distribution in the phase is random. According to chemical analysis the Al1Cr1 sample has an $Al_2O_3:Cr_2O_3$ ratio of *ca.* 1:1. According to the shifts of the unit-cell parameters with respect to the values measured for the pure phases and assuming the validity of Vegard's law,[29] found to apply quite well to the α-Cr_2O_3–α-Al_2O_3 system at high temperature,[11] we calculate an Al_2O_3 content of only 25%. This indicates either a strong deviation from Vegard's law in our low-temperature samples, or the coexistence of an alumina-rich (*ca.* 75% alumina and 25% chromia) amorphous phase with a chromia-rich corundum-type crystalline phase.

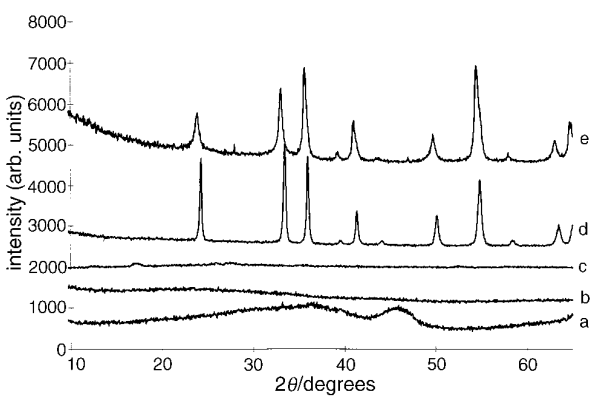

Fig. 5 XRD patterns of the mixed oxides (a) Al-400, (b) Al5Cr1-400, (c) Al2Cr1-400, (d) Al1Cr1-400, (e) Cr-400

To obtain further information on these samples, we also characterized them using FTIR and UV–VIS spectroscopy. FTFIR spectra of the mixed-oxide samples calcined at 673 K are shown in Fig. 6A. The spectrum of the Cr sample is typical for α-Cr_2O_3 powders[30,31] while that of the Al sample is typical for γ-Al_2O_3,[19,32] in agreement with XRD data. The typical sharp features of the spectrum of α-Cr_2O_3 are present, again in good agreement with XRD patterns, in the spectra of Al1Cr1, are less sharp for Al2Cr1, while they are totally absent in the spectrum of Al5Cr1. However, the position of the

Table 4 Unit-cell parameters calculated for corundum-type structures

sample	T_{calc}	phase	a/Å	c/Å	% Al_2O_3 in solid solution	
					from a	from c
eskolaite	—[a]	α-Cr_2O_3	4.954(1)	13.584(6)	—	—
Cr	673 K	α-Cr_2O_3	5.001(11)	13.693(53)	—	—
	1173 K	α-Cr_2O_3	4.973(6)	13.649(26)	—	—
Al1Cr1	673 K	α_1	4.931(2)	13.500(8)	22	24
Al1Cr1	1173 K	α_1	4.9292)	13.543(12)	23	18
Al2Cr1	673 K	α_1	4.913(8)	13.478 (48)	32	27
Al2Cr1	1173 K	α_1	4.935(9)	13.568(44)	20	13
Al5Cr1	1173 K	α_1	4.926(26)	13.595(24)	8.4	9
Al2Cr1	1173 K	α_2	4.905(11)	13.446(53)	37	33
Al5Cr1	1173 K	α_2	4.872(7)	13.458(52)	53	31
Al1Cr1	1173 K	α_3	4.845(18)	13.194(58)	68	73
Al2Cr1	1173 K	α_3	4.841(5)	13.169(22)	70	77
Al5Cr1	1173 K	α_3	4.833(8)	13.151(34)	74	80
Al	1173 K	α-Al_2O_3[b]	4.784(5)	13.027(22)	(100)	(100)
corundum	—[a]	α-Al_2O_3	4.759(1)	12.992(1)	(100)	(100)

[a]JCPDS. [b]Small amounts mixed with θ-Al_2O_3.

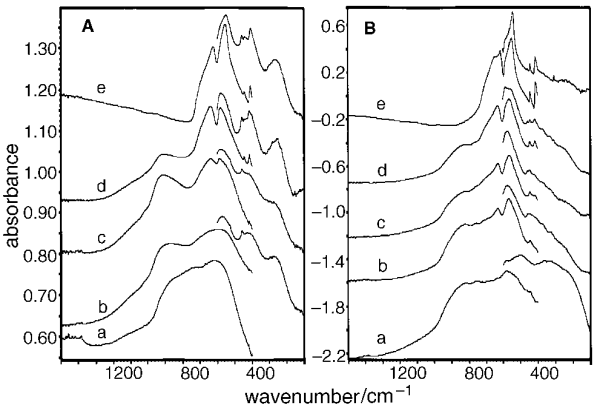

Fig. 6 FTIR/FTFIR spectra of **A**: (a) Al-400, (b) Al5Cr1-400, (c) Al2Cr1-400, (d) Al1Cr1-400, (e) Cr-400; **B**: (a) Al-900, (b) Al5Cr1-900, (c) Al2Cr1-900, (d) Al1Cr1-900, (e) Cr-900

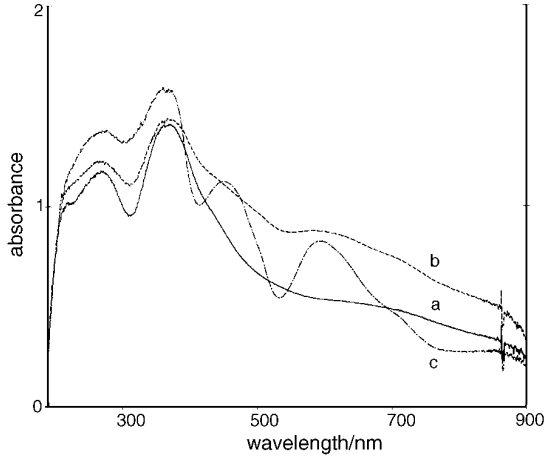

Fig. 7 Diffuse-reflectance UV–VIS spectra of (a) Al5Cr1-400, (b) Al2Cr1-400, (c) Al1Cr1-400

maxima in the mixed-oxides is markedly shifted towards higher frequencies, *i.e.* towards the peak position for α-Al_2O_3, showing, in agreement again with XRD data, a pronounced dissolution of alumina in the α-Cr_2O_3 phase.

These spectra also show broad absorption in the region 1200–600 cm^{-1}, which is typically found in aluminas with spinel-related structures[19,32] and can be assigned to vibrations of AlO_4 tetrahedra.[33] However, in this case this absorption is partly masked by a prominent band centred in the range 850–910 cm^{-1}, that can be assigned to the Cr=O stretchings of chromate ions.[34] The intensity of this band is at a maximum for the Al2Cr1 sample, where the content of the corundum-type phase is very low and the Cr content is already quite high. This is in accord with the observation that chromate species generally cover the surface of Cr^{3+}-based solids treated in air.[35–37] The presence of chromate species is also in accord with the mass losses observed at *ca.* 823 K in TG experiments.

UV–VIS spectra (Fig. 7) confirm the above data. The UV–VIS spectrum of the Al1Cr1 sample is dominated by well defined absorption bands centred at *ca.* 265, 365, 455 and 595 nm. The two higher wavelength bands both show shoulders at the higher wavenumber side, at *ca.* 500 and 710 nm. These spectra are quite similar to that of pure α-Cr_2O_3 and of chromia–alumina samples, reported and discussed previously.[3,14,38] The two split bands at 595, 710 nm and at 455, 500 nm can be assigned to the two low-energy spin-allowed d–d transitions of Cr^{3+} in an octahedral environment [$^4A_{2g}(F)\rightarrow{}^4T_{2g}(F)$ and $^4A_{2g}(F)\rightarrow{}^4T_{1g}(F)$]. Their splitting is either due to a trigonal distortion of the CrO_6 octahedra or to the appearance of additional spin-forbidden transitions, *i.e.* $^4A_{2g}(F)\rightarrow{}^2T_{1g}$ (G) and $^4A_{2g}(F)\rightarrow{}^2T_{2g}$ (G).[39] These absorptions are progressively lost in the spectra of Al2Cr1 and Al5Cr1, and are substituted by a absorption tail. This shows that Cr^{3+} species are mostly in a well characterized octahedral environment in Al1Cr1-400, as in α-Cr_2O_3, while they are in a very disordered state in Al2Cr1-400 and Al5Cr1-400.

Additionally, all three mixed Cr–Al oxide samples show absorption bands at *ca.* 265 and 365 nm that can be assigned to $O^{2-}\rightarrow Cr^{6+}$ charge-transfer transitions of chromate species.[40] Chromate ions CrO_4^{2-} typically show three very strong absorption bands, due to the three symmetry-allowed charge-transfer transitions $^1A_1\rightarrow{}^1T_2$ ($t_1\rightarrow e$), $^1A_1\rightarrow{}^1T_2$ ($t_1\rightarrow t_2$) and $^1A_1\rightarrow{}^1T_2$ ($t_2\rightarrow e$). For chromate ion in solution these absorptions are found at 366, 274 and 258 nm, so giving rise to two main absorptions as in our case, owing to the superimposition of the two higher-energy transitions.[40]

The data indicate that the calcination of the mixed Cr–Al precipitates gives rise to amorphous materials rich in chromates for Al5Cr1 and Al2Cr1, while for Al1Cr1 this amorphous phase is mixed with a highly crystalline α-Cr_2O_3-like Cr-rich phase.

Characterization of the mixed oxides produced by calcination at 1173 K

XRD patterns of the mixed oxides calcined at 1173 K are shown in Fig. 8. The XRD pattern of the pure alumina sample

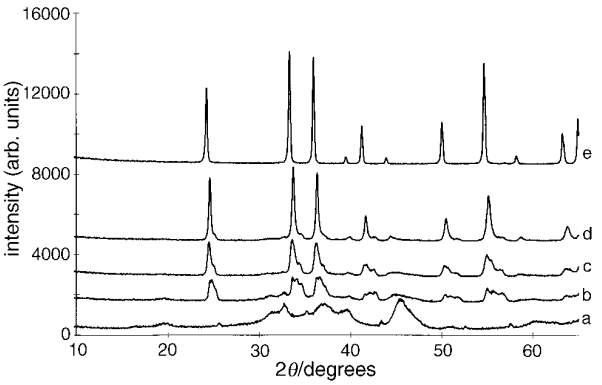

Fig. 8 XRD patterns of the mixed oxides (a) Al-900, (b) Al5Cr1-900, (c) Al2Cr1-900, (d) Al1Cr1-900, (e) Cr-900

is typical of a spinel-type phase: a γ-Al_2O_3–θ-Al_2O_3 mixture with traces of α-Al_2O_3. On the contrary, the other samples show the predominance of corundum-type phases, although small amounts of a γ-type phase can be detected in the mixed Cr–Al samples, decreasing with increasing Cr content. From the shifts of the positions of the most evident XRD peaks of such γ-type phases, *e.g.* the 400 peak (2.00 Å for pure Al_2O_3, 2.02 Å for Al5Cr1, 2.03 Å for Al2Cr1 and 2.04 Å for Al1Cr1) and the 220 peak (2.85 Å for pure Al_2O_3, 2.86 Å for Al5Cr1, 2.89 Å for Al2Cr1 and 2.88 Å for Al1Cr1) it seems likely that Cr substitutes for Al in part also in these spinel-type phases.

Interestingly, all XRD peaks of the α-type phases are split

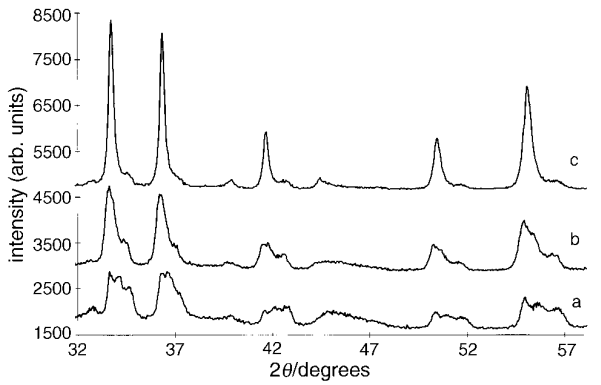

Fig. 9 XRD patterns of the mixed oxides (a) Al5Cr1-900, (b) Al2Cr1-900, (c) Al1Cr1-900 (expanded scale)

into three components, as is clearly observed in the expanded scale patterns of Fig. 9. The XRD peak position of these phases are summarized in Table 3 while the unit-cell parameters and the Al_2O_3 contents in such phases, calculated from Vegard's law, are summarized in Table 4. UV–VIS spectra of the mixed Al–Cr oxides calcined at 1173 K are dominated by the features of α-corundum-type structures, and that hexavalent Cr species only occur to a small extent and are likely to be concentrated at the surface of the powders. However, the IR spectra (Fig. 6B) show, additionally to the sharp features of α-type phases, broad bands in the region 900–700 cm^{-1} due to γ-type phases.

The XRD patterns show that a Cr-rich α-type phase (α_1) with Al_2O_3 content not exceeding 20% is predominant in the sample Al1Cr1-1173, which however also contains significant amounts of another α-type phase, rich in Al (α_3), with an Al_2O_3 content of the order of 70%. To fulfil the overall composition of the material, it is necessary to take into account that an alumina-rich γ-type phase is also present.

For the Al2Cr1-1173 sample three α-type phases are clearly present, one of which is alumina-rich (α_3, Al_2O_3 *ca.* 75%), one is Cr-rich (α_1, Al_2O_3 *ca.* 16%) and the other has an intermediate composition (α_2, Al_2O_3 *ca.* 35%). Even more evident is the formation of three α-type phases in the case of the Al5Cr1 sample, where the alumina content of the intermediate phase is *ca.* 50%.

Conclusions

The data reported above show that the probably layered mixed hydroxycarbonates of Al, Cr and ammonium can be precipitated from aqueous nitrate solutions using ammonium carbonate as the precipitant. Although this phase for the pure Al compound has already been reported[20,21] the details of the structure are, to our knowledge, unknown. We showed here that Cr can partly substitute for Al in this structure. Additional amorphous material is likely to be present especially when the Al : Cr ratio is near 1 : 1. The decomposition of these materials gives rise to complex four-phase solids. This decomposition process can be modelled following Scheme 1.

This complex decomposition pattern gives rise to different α-phases. The composition of the α_1 phase, evaluated through Vegard's law,[29] already found to apply correctly to this system,[11] is near the solubility limit measured in thermodynamically governed conditions[11] at 1173 K. On the contrary, the compositions of the α_2 and α_3 phases are very different from those measured by Sitte.[11] The appearance of solid solutions with metastable compositions can be justified by the observation that ion diffusion is low in these solids.[11]

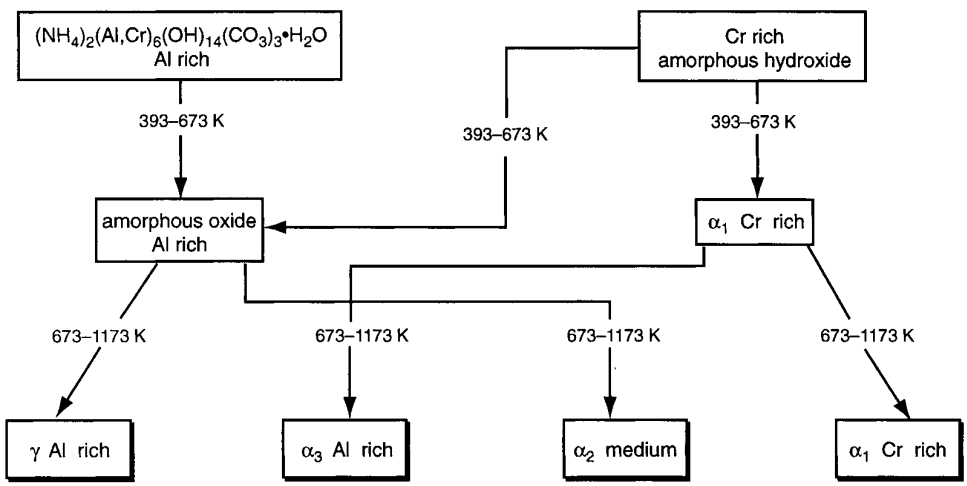

Scheme 1

Part of this work has been supported by MURST (Rome Italy) and by NATO (CRG-960316).

References

1 K. K. Kearby, in *Catalysis, Vol. III, Hydrogenation and dehydrogenation*, ed. P. H. Emmett, Reinhold, New York, 1955, p. 453.
2 D. Sanfilippo, F. Buonomo, G. Fusco, M. Lupieri and I. Miracca, *Chem. Eng. Sci*., 1992, **47**, 2313; F. Cavani and F. Trifirò, *Chim. Ind*. (*Milan*), 1994, **76**, 708; F. Cavani, M. Koutyrev, F. Trifirò, A. Bartolini, D. Ghisletti, R. Iezzi, A. Santucci and G. Del Piero, *J. Catal*., 1996, **158**, 236; S. Udomsak and R. G. Anthony, *Ind. Eng. Chem. Res*., 1996, **35**, 47.
3 C. P. Poole and D. S. McIver, *Adv. Catal*., 1967, **17**, 223.
4 R. J. Willey, H. Lai and J. B. Peri, *J. Catal*., 1991, **130**, 319.
5 A. F. Ahlström and C. U. I. Odenbrand, *Appl. Catal*., 1990, **60**, 143; S. K. Agarwal, J. J. Spivey and J. B. Butt, *Appl. Catal*., 1992, **82**, 259.
6 P. Kofstad, *High Temperature Corrosion*, Elsevier, Amsterdam, 1988.
7 A. Rousset, *J. Solid State Chem*., 1994, **111**, 164.
8 *Pigment Handbook*, ed. P. A. Lewis, Wiley, New York, 2nd edn., 1988, vol. 1.
9 A. R. West, *Solid State Chemistry and its Applications*, Wiley, New York, 1984.
10 R. M. Sprigg and S. L. Bender, *J. Am. Ceram. Soc*., 1962, **45**, 506.
11 W. Sitte, in *Reactivity of Solids*, ed. P. Barret and L. C. Dufour, Elsevier, Amsterdam, 1985, p. 451.
12 A. W. Laubengayer and H. W. McCune, *J. Am. Chem. Soc*., 1952, **74**, 2362.
13 R. J. Davis, R. H. Griffith and J. D. F. Marsh, *Adv. Catal*., 1959, **9**, 155.
14 C. Otero Areán, C. Mas Carbonell, E. Escalona Platero, F. Muñiz Macía, A. Zecchina and F. Geobaldo, *Mater. Chem. Phys*., 1993, **34**, 214.
15 G. Busca, G. Ramis, M. C. Prieto and V. Sanchez Escribano, *J. Mater. Chem*., 1993, **3**, 665.
16 M. I. Baraton, G. Busca, M. C. Prieto, G. Ricchiardi and V. Sanchez Escribano, *J. Solid State Chem*., 1994, **112**, 9.
17 M. C. Prieto, J. M. Gallardo Amores, V. Sanchez Escribano and G. Busca, *J. Mater. Chem*., 1994, **4**, 1123.
18 V. Sanchez Escribano, J. M. Gallardo Amores, E. Finocchio, M. Daturi and G. Busca, *J. Mater. Chem*., 1995, **5**, 1943.
19 G. Busca, V. Lorenzelli, G. Ramis and R. J. Willey, *Langmuir*, 1993, **9**, 1492.
20 R. F. Vogel, G. Marcelin and W. L. Kehl, *Appl. Catal*., 1984, **12**, 237.
21 G. Groppi, M. Bellotto, C. Cristiani and P. Forzatti, *J. Mater. Sci*., 1994, **29**, 3441.
22 K. Nakamoto, *Infrared and Raman spectra of Inorganic and Coordination Compounds*, Wiley, New York, 4th edn., 1986.
23 J. A. Gadsden, *Infrared Spectra of Minerals and Related Inorganic Compounds*, Butterworths, London, 1975.
24 M. C. Stegman, D. Vivien and C. Mazieres, *Spectrochimica Acta, Part A*, 1973, **29**, 1653.
25 G. Busca and V. Lorenzelli, *Mater. Chem*., 1980, **5**, 213.
26 G. Busca, V. Lorenzelli and V. Sanchez Escribano, *Chem. Mater*., 1992, **4**, 595.
27 S. J. Wilson and J. D. C. McConnell, *J. Solid State Chem*., 1980, **34**, 315.
28 R. S. Zhou and R. L. Snyder, *Acta Crystallogr., Sect. B*, 1991, **47**, 617.
29 A. R. West, *Solid State Chemistry and its Applications*, Wiley, New York, 1984, p. 367.
30 R. Marshall, S. S. Mitra, P. J. Gielisse, J. N. Plendl and C. Mansur, *J. Chem. Phys*., 1965, **43**, 2893.
31 C. J. Serna, J. L. Rendon and J. E. Iglesias, *Spectrochim. Acta, Part A*, 1982, **38**, 797.
32 G. A. Dorsey, *Anal. Chem*., 1968, **40**, 971.
33 P. Tarte, *Spectrochim. Acta, Part A*, 1967, **23**, 2127.
34 O. Muller, W. B. White and R. Roy, *Spectrochim. Acta, Part A*, 1969, **25**, 1491.
35 A. Zecchina, S. Coluccia, E. Guglielminotti and G. Ghiotti, *J. Phys. Chem*., 1971, **75**, 2774, 2783, 2790.
36 K. Hadjiivanov and G. Busca, *Langmuir*, 1994, **10**, 4534.
37 R. J. Willey, P. Noirclerc and G. Busca, *Chem. Eng. Commun*., 1993, **123**, 1.
38 G. Munuera, P. Valerga and V. Rives, *Ceramica y Vidrio*, Universidad de Sevilla, Serie Ciencia, 1978, vol. 21, p. 73.
39 M. Lenglet, M. Bizi and C. K. Jorgensen, *J. Solid State Chem*., 1990, **86**, 82.
40 Z. G. Szabo, K. Kamaras, Sz. Szebeni and I. Ruff, *Spectrochim. Acta, Part A*, 1978, **34**, 607.

Paper 7/01344B; *Received* 26*th February*, 1997